S. I. – CEC FRAMEWORK

Use of GIS-AHP tools for potable groundwater potential zone investigations—a case study in Vairavanpatti rural area, Tamil Nadu, India

Prabakaran Kulandaisamy [1] (ID) · Sivakumar Karthikeyan [1] (ID) · Aruna Chockalingam [1]

Abstract

Vairavanpatti is a rural area in the district of Sivagangai, Tamil Nadu, India, prone to water deficiency. Azimuthal square array for vertical electrical sounding (VES) techniques were used to delineate the geoelectrical layers at five different locations. Groundwater samples were collected in 15 locations and analyzed for pH, EC, TDS, TH, T-Alk, Ca, Cl, SO_4, Fe, and SiO_2 levels. The minimum and maximum apparent resistivity values recorded in location 5 with 37.6 Ωm and location 4 with 1150.7 Ωm. Most of the quality parameters exceeds the WHO (2008) and BIS (2012) guideline values except pH and SO_4. Iso-resistivity maps for apparent resistivity values suggest at 10-m intervals a total depth of 80 m. The iso-resistivity maps and spatial distribution maps were reclassified with respect to their desired values based on WHO (2008) and BIS (2012) guidelines for drinking water. Analytical hierarchy processes (AHPs) were used to assign the weights for each reclassified layers. The relative importance of layers for potable groundwater and potential zone were identified, in which the consistency ratio is kept as below 0.1. The result shows that the 23% groundwater of northern part is not suitable for drinking purposes. In the overall study area, 51.33% of the southwest, southeast, and central parts possess potable groundwater with moderate potential. In northern part, 22.42% have non-potable and moderate potential while 13.38% of the northeastern part contains good potential of potable groundwater. All other categories are 12.21% of potable and poor potential, 0.5% of non-potable with good potential, and 0.16% of non-potable with poor potential of groundwater in the study area. Rainwater harvesting and artificial recharge must be implemented in these areas to improve the potential and quality of groundwater. It is understood that AHP-enabled GIS can be used effectively in the identification of potable and potential groundwater zone in any complex regions.

Keywords Groundwater · Major ions · Quality · VES · AHP and GIS

Introduction

Groundwater investigation is given more significance due to water scarcity in India and for the ever-growing demand for water provisions, particularly in areas with insufficient surface water resources. Ten percent of the world's population is exaggerated by chronic water shortage, and this is expected to increase one third by 2025 (WHO 1996). Since, the industrial insurgency, detailed studies on natural water systems, and polluted waters have been given more importance in every part of the globe (Mohamed et al. 2009; Juahir et al. 2011; Sivakumar et al. 2016; Ramachandran et al. 2020; Chung et al. 2020). The rising freshwater crisis in terms of quality and quantity is already felt in India due to the contamination of freshwater resources, more drafting of groundwater, and declining trends of surface water during summer, and it has urged the need for a thorough study on the quality and quantity of groundwater in different parts of India (Selvam et al. 2016; Sivakumar et al. 2017; Ravindran et al. 2018; Kanagaraj et al. 2019; Chandra et al. 2019). Nature of groundwater depends on the rock-water interaction in aquifer systems. The searching of groundwater is faced with lots of uncertainties; to minimize or avoid failures altogether, it is pertinent that the

✉ Sivakumar Karthikeyan
siva.karthi90@yahoo.com

[1] Department of Geology, Faculty of Science, Alagappa University, Karaikudi 630003, India

right exploration techniques are utilized in the definition of subsurface water-bearing formations (Coker et al. 2009).

The great advances in geophysics during the last two decades altered not only the field equipment and practice but also the advanced interpretation techniques. The new electronic devices and widespread application of digital computers are used to interpret the geophysical data. The quality of water, as well as quantity, is an essential concern since it is directly linked to plant growth and human health (Hem 1991; Karanth 1997). Water quality gets modified based on the various hydrological cycle process such as evaporation, transpiration, and selective uptake by vegetation, oxidation/reduction, cation exchange, dissociation of minerals, precipitation of secondary minerals, mixing of waters, leaching of fertilizers and manure, pollution, and biological processes (Appelo and Postma 2005). The hydrochemical knowledge is vital in determining the source and composition of groundwater (Zaporozec 1972).

Physicochemical parameters are necessary for assessing the suitability of water for various purposes like drinking, domestic, agricultural, and industrial. Many studies in different parts of India have been carried out on groundwater quality deterioration with respect to drinking domestic and irrigation purposes (Majumdar and Gupta 2000; Dasgupta and Purohit 2001; Khurshid et al. 2002; Sujatha and Redd 2003; Pulle et al. 2005; Subba Rao 2006). Some of the common geochemical processes that control the physicochemical parameters of the aquifer water are evaporation, deposition, dissolution, weathering of minerals, and ion exchange. These processes are also responsible for the seasonal and spatial variations of groundwater chemistry. The quality of waters is influenced by rainfall patterns, surface characteristics, land use, soils, and geology of the areas. Detailed knowledge of the hydrogeochemical process that control chemistry is very essential to understand and deal with the groundwater-associated problems. The continuous monitoring of groundwater to know the variation in its chemical composition and the graphical analyses of hydro-geochemical data helps to determine the hydrogeochemical processes of a particular region. Thus, the hydrogeochemical studies will assist in planning and in taking counteractive actions to protect aquifers that are contaminated by natural and as well as anthropogenic activities (Chidambaram et al. 2012, 2013; Chandrasekar et al. 2013; Krishna kumar et al. 2014). Geographic information system (GIS) is a potential tool to address the issues in water resource like quality assessment and management for regional as well as local scale and used to develop the solutions for water-related problems (Gnanachandrasamy et al. 2015; Selvam et al. 2016; Venkatramanan et al. 2017). Analytical hierarchy process (AHP), developed by Saaty in 1980, is a well-known method and widely used in multi-criteria analysis with integrated pairwise comparison matrix to calculate the weights of each criteria for decision-making problems

(Cabrera and Lee 2019). In recent years, researchers from all over the globe use the AHP with GIS in natural hazard vulnerability mapping and various environmental suitability studies (Machiwal et al. 2011; Mondal 2012; Rahimi and Mokarram 2012; Ajin et al. 2014; Fenta et al. 2014; Selvam et al. 2015; Gangadharan et al. 2016; Ibrahim et al. 2017; Pinto et al. 2017). The main theme of this work is to elucidate through geoelectrical methods to measure the subsurface formations, and to know the groundwater potential zones with new comprehensive techniques for the identification potable groundwater potential zones (PGWPZ), based on the multi-criteria analysis in GIS enabled with AHP. This study overlays the spatial distribution of geophysical and geochemical data to delineate the potential groundwater zones, which in turn could be used for adequate management and decision-making schemes.

Study area

Vairavanpatti is situated to the southeast of Sivagangai district, Tamil Nadu, India (Fig. 1). This region is located between 78° 39′ 12.6″ E and 78° 39′ 50.04″ E latitudes–10° 07′ 21″ N and 10° 08′ 2.4″ N longitudes, and it covers 150 acres (0.6 km^2) of groundwater-based agriculture land. The annual rainfall ranges from 861 to 988 mm with an average of 905 mm, and it prevails 60 to 75% of high relative humidity throughout the year. Southwest and northeast monsoons are the seasons when the study area get its rainfall in which northeast monsoon contributes more precipitation than the southwest monsoon (CGWB 2008). There are two tanks available in the study area which are fed by rainwater, and the water stored in these tanks is used for irrigation when they filled mostly in rainy seasons. The geology of this region is consists of garnetified charnockite, mica schist, granite gneiss, and granites associated with intrusive rocks of Archean age. The area is highly undulated, due to the irregular weathering conditions. Weathering thickness and interconnected regional fractures make the wells to be productive in this region. The groundwater condition in a terrain is highly variable depending on the weathering, fracturing regional groundwater flow, and local withdrawal pattern. The groundwater condition is mainly influenced by soil cover, which controls the local vertical recharge of rainwater. The top soil of the study area is composed of iron-enriched red loam which is derived from the granitic host rocks. The thickness of the weathered and jointed rock decides the total groundwater storage while the opening in the fractures controls the movement of water in the subsurface. Distinct drainage futures could not be identified due the small scale of the study area. The groundwater condition can be studied in microlevel by studying the
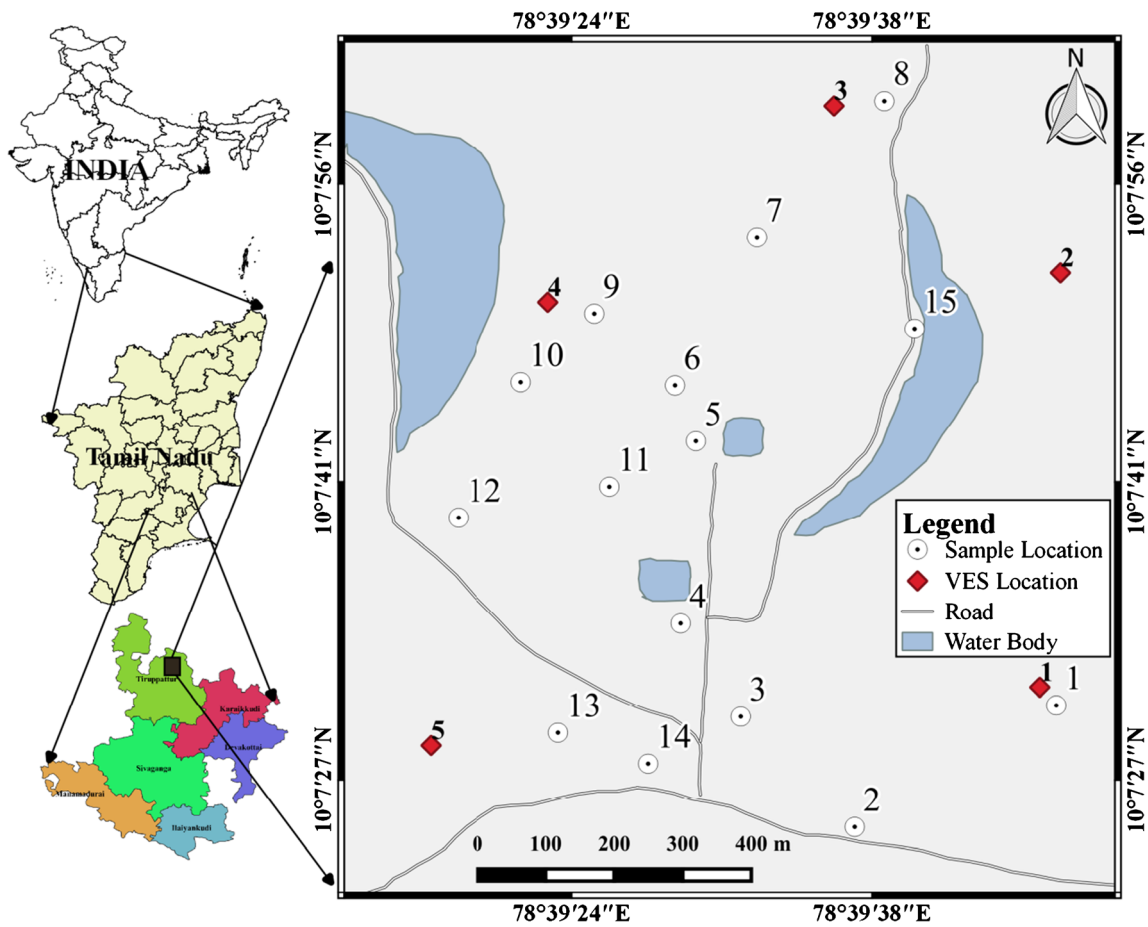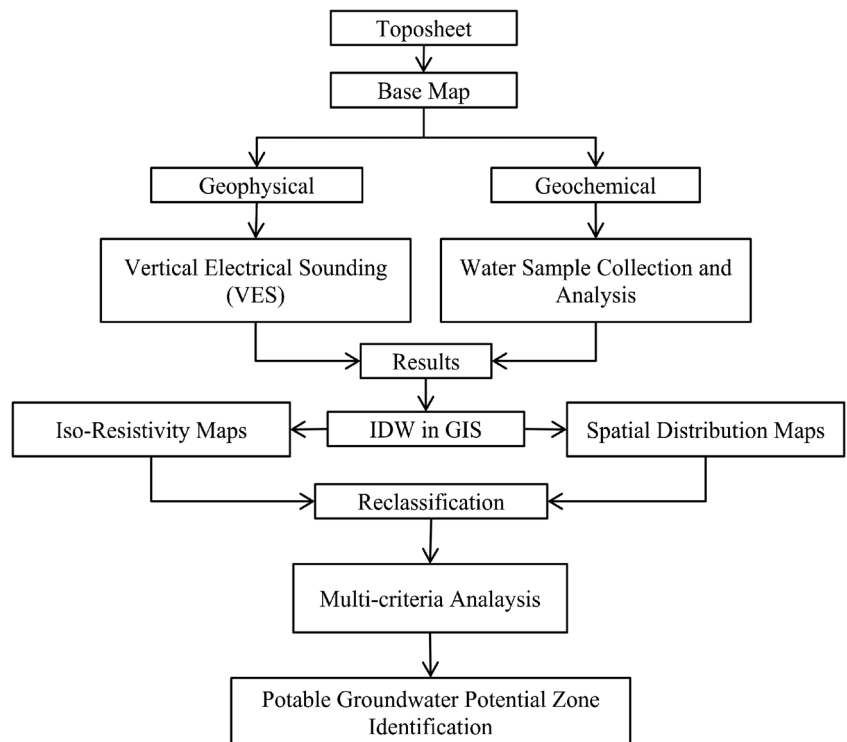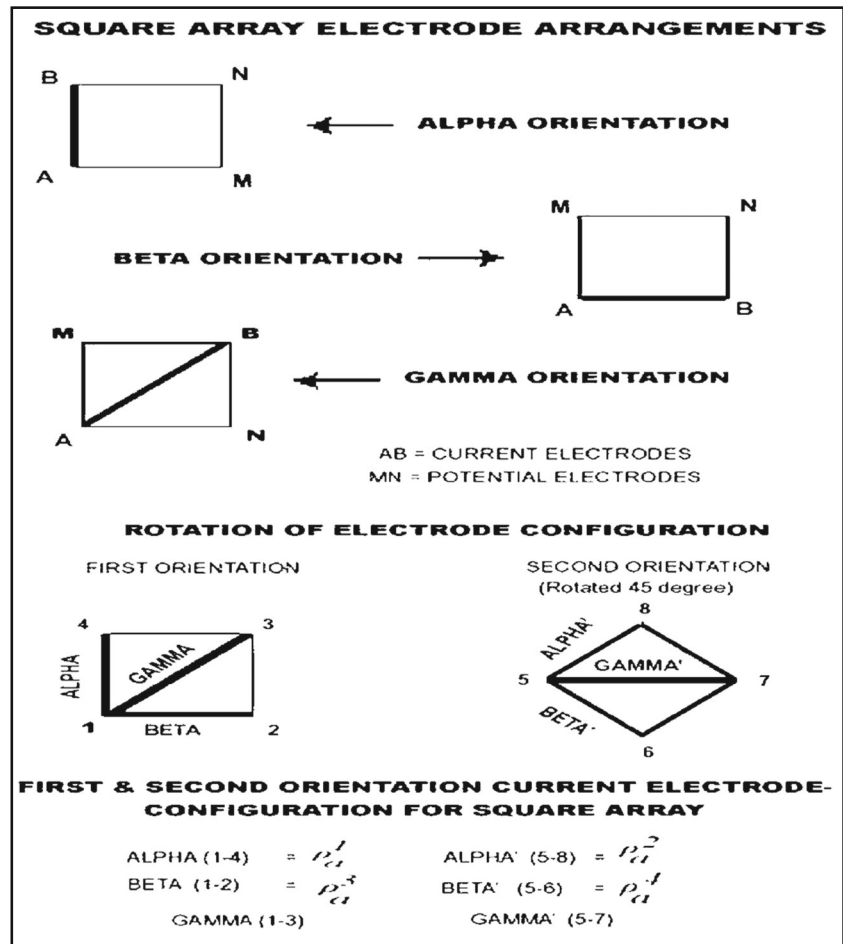
Fig. 1 Groundwater samples and VES locations of Vairavanpatti, Southern India

Fig. 2 Methodology flowchart

Fig. 3 Electrode arrangements of square array method (after Ravindran 2012)

available well water levels, weathered portion thickness, joint type, and fractures in the host rocks. The geophysical surveys are helpful in demarcating the weathered zones, the nature of the fracture system, the regional structural features, and the presence of the deep fractures of particular region.

Table 1 Apparent resistivity (in Ωm) values of vertical electrical soundings

Sl. no.	AB/2 in (m)	Lat. 10.1254° Long. 78.6627° VES 1 Ωm	Lat. 10.1256° Long. 78.6629° VES 2 Ωm	Lat. 10.1247° Long. 78.6619° VES 3 Ωm	Lat. 10.1250° Long. 78.6628° VES 4 Ωm	Lat. 10.1255° Long. 78.6619° VES 5 Ωm
1	10	78.9	61.0	97.8	62.2	37.6
2	20	131.4	51.5	256.0	569.6	143.6
3	30	234.9	162.0	203.7	89.6	110.5
4	40	161.0	216.5	320.7	55.7	345.2
5	50	817.4	236.0	362.1	93.8	577.8
6	60	890.5	313.0	430.9	567.9	519.1
7	70	322.7	353.5	502.4	1150.7	316.3
8	80	521.8	365.0	606.3	478.5	940.8
9	90	867.8	–	754.0	555.7	–
10	100	–	–	768.1	403.6	–
Minimum		78.9	51.5	97.8	55.7	37.6
Maximum		890.5	365.0	768.1	1150.7	940.8
Mean		447.4	219.8	430.2	402.7	373.9

Table 2 Results of physicochemical parameters for drinking purposes

S. no.	Latitude in decimal	Longitude in decimal	pH	EC	TDS	T-Alk	TH	Ca	Cl	SO$_4$	Fe	SiO$_2$
1	10.125	78.663	7.0	1290	864	264	386	232	142	102	0.28	71
2	10.123	78.660	6.7	1450	972	352	452	268	185	46	0.09	116
3	10.125	78.659	8.4	910	610	432	52	32	131	24	0.07	46
4	10.126	78.658	6.7	1740	1166	312	556	335	256	44	0.17	101
5	10.129	78.658	7.0	1260	844	360	430	256	102	31	0.18	101
6	10.129	78.658	6.8	2200	1474	416	512	300	264	78	0.56	105
7	10.131	78.659	6.7	2596	1741	355	824	479	319	106	0.22	72
8	10.133	78.661	6.5	1920	1286	235	525	320	272	77	0.27	50
9	10.130	78.657	6.7	1750	1173	325	475	285	165	98	0.72	55
10	10.129	78.656	7.8	550	369	225	215	105	17	18	0.40	95
11	10.128	78.657	7.0	640	429	260	240	140	35	12	0.44	91
12	10.128	78.655	7.4	820	549	320	300	185	49	21	0.34	68
13	10.125	78.656	7.6	840	563	164	210	130	96	60	0.06	6
14	10.124	78.658	7.5	461	308	120	146	120	35	10	0.27	16
15	10.130	78.661	7.4	980	657	120	300	224	173	20	0.31	12
Minimum			6.5	461	308	120	52	32	17	10	0.06	6
Maximum			8.4	2596	1741	432	824	479	319	106	0.72	116
Mean			7.1	1294	867	284	375	227	149	50	0.29	67
WHO (2008) and (BIS 2012) guideline values			6.5–8.5	1500	500–2000	20–200	200–600	75–200	250–1000	200–400	0.3	–

*Units for each parameter: pH has no unit, EC in μS/cm, all other parameters are in ppm

Methodology

The methodology adopted for this study to accomplish the objective can be divided into three major parts. They are (1) vertical electrical sounding (VES) using azimuthal square array and groundwater sampling, (2) interpretation of electrical resistivity method and groundwater sample analysis for the physicochemical parameters, and (3) potable groundwater potential zone identification using multi-criteria analysis in GIS and AHP (Fig. 2). VES using the square array method (Fig. 3) is used by

Aquameter (CRM500) resistivity meter (Table 1). Portable unit of Aquameter CRM 500 is a high power version (40 W) which is useful for any type of soil, and it has automatic Earth current setting and rechargeable batteries. In square array method, the apparent resistivity values are taken by fixing the current and potential electrodes in three different orientations as given in the Fig. 3 (Ravindran 2012). Groundwater samples were collected at 15 locations in summer season in the year of 2019 (Table 2). Clean polyethylene bottles of 1-L capacity were used to collect and store water samples. The bottles

Table 3 Correlation matrix for analytical results

Parameters	pH	EC	TDS	T-Alk	TH	Ca	Cl	SO$_4$	Fe	SiO$_2$
pH	1.00									
EC	−0.71	1.00								
TDS	−0.71	*1.00*	1.00							
T-Alk	−0.15	0.51	0.51	1.00						
TH	−0.83	*0.92*	*0.92*	0.35	1.00					
Ca	−0.84	*0.90*	*0.90*	0.27	*0.99*	1.00				
Cl	−0.61	*0.94*	*0.94*	0.37	*0.82*	*0.83*	1.00			
SO$_4$	−0.58	*0.80*	*0.80*	0.29	*0.71*	0.68	0.68	1.00		
Fe	−0.30	0.15	0.15	0.04	0.15	0.14	−0.04	0.22	1.00	
SiO$_2$	−0.43	0.33	0.33	*0.65*	0.41	0.33	0.17	0.07	0.14	1.00

Significant positive correlation of r>60 is denoted as italic form

Table 4   Preference scale between two criteria as used in AHP (Saaty 1980)

Scale	Degree of preference	Explanation
1	Equally	Two criteria contribute equally to the objective
3	Moderately	Experience and judgment slightly-to-moderately favor one criterion over another
5	Strongly	Experience and judgment strongly or essentially favor one criterion over another
7	Very strongly	A criterion is strongly favored over another and its dominance is showed in practice
9	Extremely	The evidence of favoring one criterion over another is of the highest degree possible of an affirmation
2, 4, 6, 8	Intermediate values	Used to represent compromises between the preferences in weights 1, 3, 5, 7, and 9
1/any of the scale value	Reciprocals of above nonzero values	If criteria i has one of the above nonzero numbers assigned to it when compared with criteria j, then j has the reciprocal value when compared with I and the degree of preferences will change according to the value.

were pre-rinsed with distilled water to avoid the contamination error and rinsed with water before collecting the samples. Groundwater samples were collected 30 cm below the water level in open wells using buckets while samples were collected in borewells after few minutes of pumping. pH, electrical conductivity (EC), and total dissolved solids (TDS) were measured using portable meters (PCSTestr 35) in the field. Longitude and latitude of each VES location and each sampling well were noted down using the portable GPS device (GARMIN GPS) (Tables 1 and 2). Samples were analyzed in the laboratory for water quality parameters such as total alkalinity (T-Alk), total hardness (TH), calcium (Ca), chloride (Cl), sulfate (SO_4), iron (Fe), and silicate (SiO_2) using standard procedures of APHA 1995. Correlation matrix for the analytical results are given in the Table 3 followed by analytical hierarchy process (Tables 4, 5, 6, 7, 8 and 9). Iso-resistivity maps were prepared for the depth wise apparent resistivity values and physicochemical parameters interpolated with inverse distance weighted (IDW) spatial techniques in QGIS 2.8 (Venkatramanan et al. 2015; Gnanachandrasamy et al. 2018). The iso-resistivity maps and spatial distribution maps were reclassified based on desired values (Tables 10 and 11)

for potable groundwater potential zones. All the reclassified layers are incorporated in AHP in QGIS 2.8 of Saga Module (Conrad et al. 2015; Selvam et al. 2015).

Results and discussion

Geophysics

Depth wise apparent resistivity was obtained by varying spacing between 10 and 100 m, at an interval of 10 m which is given in the Table 1. Low apparent resistivity value is obtained from VES profile 5 followed by VES nos. 2, 4, 1, and 3; high apparent resistivity is obtained from profile 4 followed by VES nos. 5, 1, 3, and 2. The order of mean apparent resistivity is $1 > 3 > 4 > 5 > 2$. Vertical electrical cross section of the VES profiles is shown in Fig. 4. It clearly shows that the location 2 is having more possibilities for potential groundwater zone due to its low resistivity in deeper depths compared to other profiles (Habberjam and Watkins 1967; Habberjam 1972, 1975, 1979; Ravindran 2012; Ravindran et al. 2018), whereas VES 1 and 4 are devising lesser

Table 5 Pairwise comparison matrix of the eight iso-resistivity layers

Layers	Depth 1	Depth 2	Depth 3	Depth 4	Depth 5	Depth 6	Depth 7	Depth 8
Depth 1	1.000	0.333	0.200	0.200	0.143	0.143	0.111	0.111
Depth 2	3.000	1.000	0.333	0.333	0.200	0.143	0.143	0.111
Depth 3	5.000	3.000	1.000	0.333	0.200	0.200	0.143	0.143
Depth 4	5.000	3.000	3.000	1.000	0.333	0.333	0.200	0.200
Depth 5	7.000	5.000	5.000	3.000	1.000	0.333	0.200	0.143
Depth 6	7.000	7.000	5.000	3.000	3.000	1.000	0.333	0.200
Depth 7	9.000	7.000	7.000	5.000	5.000	3.000	1.000	0.200
Depth 8	9.000	9.000	7.000	5.000	7.000	5.000	5.000	1.000
Sum	46.000	35.333	28.533	17.867	16.876	10.152	7.130	2.108

Table 6 The normalized eigenvector for comparison matrix of iso-resistivity layers

Layers	Depth 1	Depth 2	Depth 3	Depth 4	Depth 5	Depth 6	Depth 7	Depth 8	Weights
Depth 1	0.022	0.009	0.007	0.011	0.008	0.014	0.016	0.053	0.018
Depth 2	0.065	0.028	0.012	0.019	0.012	0.014	0.020	0.053	0.028
Depth 3	0.109	0.085	0.035	0.019	0.012	0.020	0.020	0.068	0.046
Depth 4	0.109	0.085	0.105	0.056	0.020	0.033	0.028	0.095	0.066
Depth 5	0.152	0.142	0.175	0.168	0.059	0.033	0.028	0.068	0.103
Depth 6	0.152	0.198	0.175	0.168	0.178	0.098	0.047	0.095	0.139
Depth 7	0.196	0.198	0.245	0.280	0.296	0.295	0.140	0.095	0.218
Depth 8	0.196	0.255	0.245	0.280	0.415	0.492	0.701	0.474	0.382
Eigenvector	1.000	1.000	1.000	1.000	1.000	1.000	1.000	1.000	1.000

possibilities for groundwater as the higher resistivity encountered, which is due to the presence of massive rock formations. Iso-resistivity maps illustrate the spatial distribution of apparent resistivity values noted at 10-m intervals up to 80-m depth from the surface (Figs. 5 and 6). The heterogeneity of the subsurface formations due to the irregular weathering and fracturing results in the uneven apparent resistivity for the layers that revealed in the iso-resistivity maps.

Geochemistry

The groundwater analytical results are shown in the Table 2, in which most of the parameters exceed the WHO (2008) and BIS (2012) guideline values except pH, SO_4, and SiO_2. Box and Whiskers plot (Fig. 7) show the variable distribution within minima and maxima of the parameters. Significant positive correlation of $r > 60$ is found between the parameters EC, TDS, TH, Ca, Cl, and SO_4.

The T-Alk shows positive correlation of above 60 with SiO_2 in groundwater, whereas no mutual correlation was recorded by pH and Fe with other parameters which reveal that pH and Fe are independent (Table 3). The spatial distribution of the obtained results and the respective reclassifed layers are shown in the Figs. 8 and 9.

Hydrogen ion activity (pH)

The regional distribution of groundwater pH is shown in the Fig. 8 (pH). Groundwater pH varies between 6.5 and 8.4 with an average of 7.1, and it is having an increasing trend in southern direction; it may be due to overpumping from deeper aquifers tending to increase the influence of the highly saturated groundwater. The maximum value of pH 8.4 was recorded in the sample number 3, which did not exceeded the WHO 2008 guideline value for drinking water.

Table 7 Pairwise comparison matrix of water quality parameters

Parameters	pH	EC	TDS	TH	T-Alk	Ca	Cl	SO_4	Fe	SiO_2
pH	1.000	0.333	0.333	0.333	0.200	0.200	0.143	0.143	0.111	3.000
EC	3.000	1.000	1.000	0.333	0.333	0.333	0.200	0.143	0.111	3.000
TDS	3.000	1.000	1.000	0.333	0.333	0.200	0.200	0.143	0.111	3.000
TH	3.000	3.000	3.000	1.000	0.333	0.333	0.200	0.200	0.143	3.000
T-Alk	5.000	3.000	3.000	3.000	1.000	0.333	0.333	0.200	0.143	3.000
Ca	5.000	3.000	5.000	3.000	3.000	1.000	0.333	0.200	0.200	9.000
Cl	7.000	5.000	5.000	5.000	3.000	3.000	1.000	5.000	0.333	9.000
SO_4	7.000	7.000	7.000	5.000	5.000	5.000	0.200	1.000	0.200	9.000
Fe	9.000	9.000	9.000	7.000	7.000	5.000	3.000	5.000	1.000	9.000
SiO_2	0.333	0.333	0.333	0.333	0.333	0.111	0.111	0.111	0.111	1.000
Sum	43.333	32.667	34.667	25.333	20.533	15.511	5.721	12.140	2.463	52.000

Table 8 The normalized eigenvector for comparison matrix of spatial distribution layers

Parameters	pH	EC	TDS	TH	T-Alk	Ca	Cl	SO₄	Fe	SiO₂	Weights
pH	0.023	0.010	0.010	0.013	0.010	0.013	0.025	0.012	0.045	0.058	0.022
EC	0.069	0.031	0.029	0.013	0.016	0.021	0.035	0.012	0.045	0.058	0.033
TDS	0.069	0.031	0.029	0.013	0.016	0.013	0.035	0.012	0.045	0.058	0.032
TH	0.069	0.092	0.087	0.039	0.016	0.021	0.035	0.016	0.058	0.058	0.049
T-Alk	0.115	0.092	0.087	0.118	0.049	0.021	0.058	0.016	0.058	0.058	0.067
Ca	0.115	0.092	0.144	0.118	0.146	0.064	0.058	0.016	0.081	0.173	0.101
Cl	0.162	0.153	0.144	0.197	0.146	0.193	0.175	0.412	0.135	0.173	0.189
SO4	0.162	0.214	0.202	0.197	0.244	0.322	0.035	0.082	0.081	0.173	0.171
Fe	0.208	0.276	0.260	0.276	0.341	0.322	0.524	0.412	0.406	0.173	0.320
SiO₂	0.008	0.010	0.010	0.013	0.016	0.007	0.019	0.009	0.045	0.019	0.016
Eigenvector	1.000	1.000	1.000	1.000	1.000	1.000	1.000	1.000	1.000	1.000	1.000

Electrical conductivity (EC)

The flow of electrical current through the water is based on the salt content of the water, and the measurement of the flowing current is denoted as electrical conductivity (EC) of the water. In general, the higher the salt content, the greater the flow of electrical current. EC is expressed as μS/cm and is reciprocal of resistivity (R). Figure 8 (EC) shows the clear picture of the spatial distribution of the EC value in the study area. The minimum, maximum, and mean EC values of the groundwater sample are 461, 2596, and 1294 μS/cm. The regional distribution of EC is similar to that of TDS though both are interrelated variables. Higher EC is found in the northern part; it may be due to the rock water interaction which increases the dissolved solid content in this region. Thirty-three percent of the groundwater samples exceed the WHO 2008 guideline value of 1500 μS/cm for drinking purpose.

Total dissolved solids (TDS)

The TDS values are varying between 308 and 1741 ppm with an average value of 867 ppm in the study area. The WHO (2008) and (BIS 2012) permissible limits are 1000 and 2000 ppm, and the acceptable limit is 500 ppm for drinking water. Groundwater samples of 10, 11, and 14 are measured as below 500 ppm for TDS, making them suitable for drinking. The spatial distribution of TDS concentration in groundwater is presented in Fig. 8 (TDS). The TDS is very high in the northeastern part, and it may be due to the dissolution of the elements from the aquifer media (Chidambaram et al. 2013).

Total alkalinity (T-Alk)

The alkalinity values range from 120 to 432 ppm with an average value of 284 ppm. Carbonates, phosphates, and hydroxides are the common materials present in water to increase the alkalinity. Figure 8 (T-Alk) shows the spatial pattern of the alkalinity values in which the northeast and southwest parts recorded low alkalinity. Twenty to 200 ppm is the acceptable to permissible range for alkalinity in drinking water as per WHO (2008) and BIS (2012). Three samples (13, 14, and 15) fall under the permissible limit for total alkalinity.

Table 9 The consistency evaluation of weights derived in AHP

Consistency evaluation	Iso-resistivity layers	Quality parameters
$\lambda max = \sum_{i=1}^{n} X_{i,j} \times W_{i,j}$	8.046	11.331
Consistency index (CI) $= \frac{\lambda - n}{n-1}$	0.007	0.148
Random index (RI) (by Saaty 1980)	1.41 ($n = 8$)	1.49 ($n = 10$)
Consistency ratio (CR) $= \frac{CI}{RI}$	0.005	0.099
$CR < 0.10$ so the weights are consistent		

Table 10 Assigned weights for the reclassified iso-resistivity layers after AHP

Depth	Range (Ωm)	Score	Weights	Depth	Range (Ωm)	Score	Weights
10 m	37–61	3	0.018	50 m	93–236	3	0.103
	61–78	2			236–577	2	
	78–98	1			577–818	1	
20 m	51–131	3	0.028	60 m	313–430	3	0.139
	131–256	2			430–567	2	
	256–569	1			567–891	1	
30 m	89–110	3	0.046	70 m	316–353	3	0.218
	110–203	2			353–502	2	
	203–235	1			502–1151	1	
40 m	55–216	3	0.066	80 m	365–478	3	0.382
	216–320	2			578–606	2	
	320–346	1			606–941	1	

Total hardness (TH)

Total hardness (TH) of groundwater was calculated by TH (ppm) = 2.497Ca + 4.115 mg (Sawyer and McCarty 1978). So that the spatial pattern of TH values are almost similar to the Ca spatial pattern. The hardness values range from 52 to 824 ppm with an average value of 375 ppm during water hardness. The maximum tolerable limit of TH for drinking is 600 ppm, and the most desirable limit is 200 ppm as per the BIS standard. Very hard category water is present in the northern part of the study area (Fig. 8 (TH)).

Calcium (Ca)

Generally, in the Earth's crust, many rock-forming minerals contain calcium as a major constituent; it is the most abundant alkaline element in the Earth's crust with extreme mobility in hydrosphere. The groundwater calcium is varied from 32 to 479 ppm, with an average of 227 ppm. From the spatial diagram (Fig. 8 (Ca)), it is observed that the calcium concentration is high in the northern part and has decreasing trend towards the southern part which is due to the recharging water dissolving the calcium-rich feldspars from the granitic rocks (Chidambaram et al. 2013). All the groundwater samples exceed the acceptable limit of 75 ppm (WHO 2008) except sample no. 3, and 60% of them exceed the permissible limit of 200 ppm as per BIS (2012).

Chloride (Cl)

Chloride ion is a major dissolved anion of most natural waters, though it is a minor constituent of the Earth's crust. The chloride concentration alone indicates the quality of water primarily. Figure 8 (Cl) shows the chloride's spatial distribution pattern in this region, and it varies from 17 to 319 ppm with an average value of 149 ppm. It is observed that the chloride concentration is high in the northern part and low in the southern part. Twenty-seven percent of the groundwater is unsuitable for drinking because it exceeds the WHO (2008) guideline value of 250 ppm.

Table 11 Assigned weights for the reclassified spatial layers of quality parameters after AHP

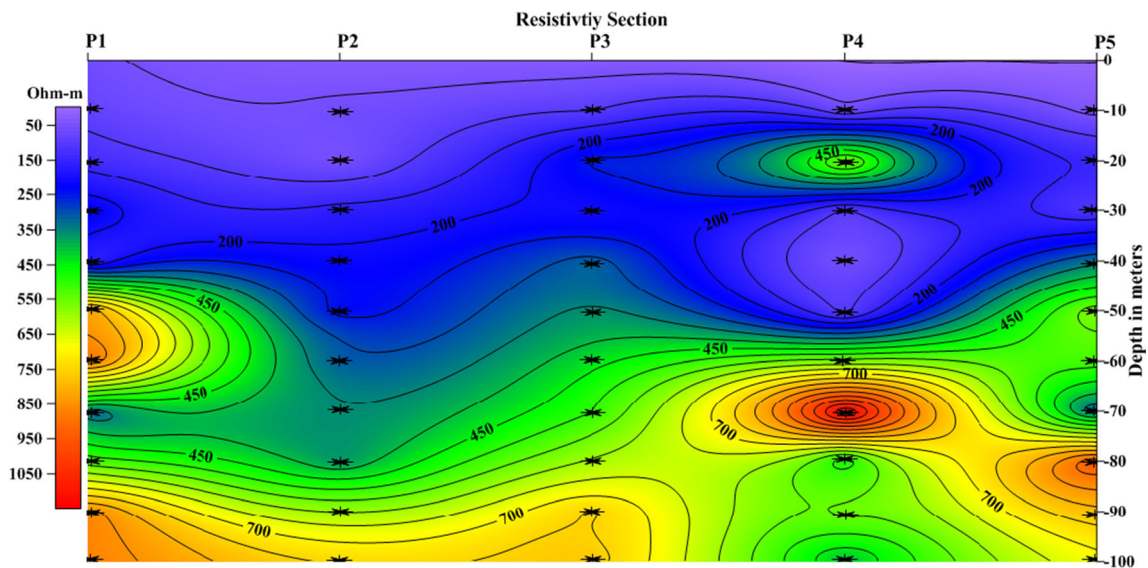| Parameters	Range	Boolean logic	Weights	Parameters	Range	Boolean logic	Weights
pH	6.5–8	0	0.022	Ca	32–200	0	0.101
	8–8.5	1			200–480	1	
EC	461–1500	0	0.033	Cl	17–200	0	0.189
	1500–2600	1			200–320	1	
TDS	308–1000	0	0.032	SO$_4$	10–80	0	0.171
	1000–1800	1			80–106	1	
TH	52–200	0	0.049	Fe	0.06–0.3	0	0.32
	200–825	1			0.3–0.72	1	
T-Alk	120–200	0	0.067	SiO$_2$	6–30	0	0.016
	200–432	1			30–116	1	

Fig. 4 Vertical cross section of the electrical sounding

Sulfate (SO₄)

Sulfate concentration varies from 10 to 106 ppm, with an average value of 50 ppm in groundwater of this area. The spatial variation of sulfate concentration in this area is influenced by the cultivation pattern. Figure 8 (SO₄) shows that the higher concentration of sulfate is observed in the northern and southeastern parts and small pockets of low sulfate regions are also observed in the central, southern, and western parts. However, the SO_4 concentration does not exceed the WHO (2008) and BIS (2012) acceptable limit of 200 ppm for drinking water quality.
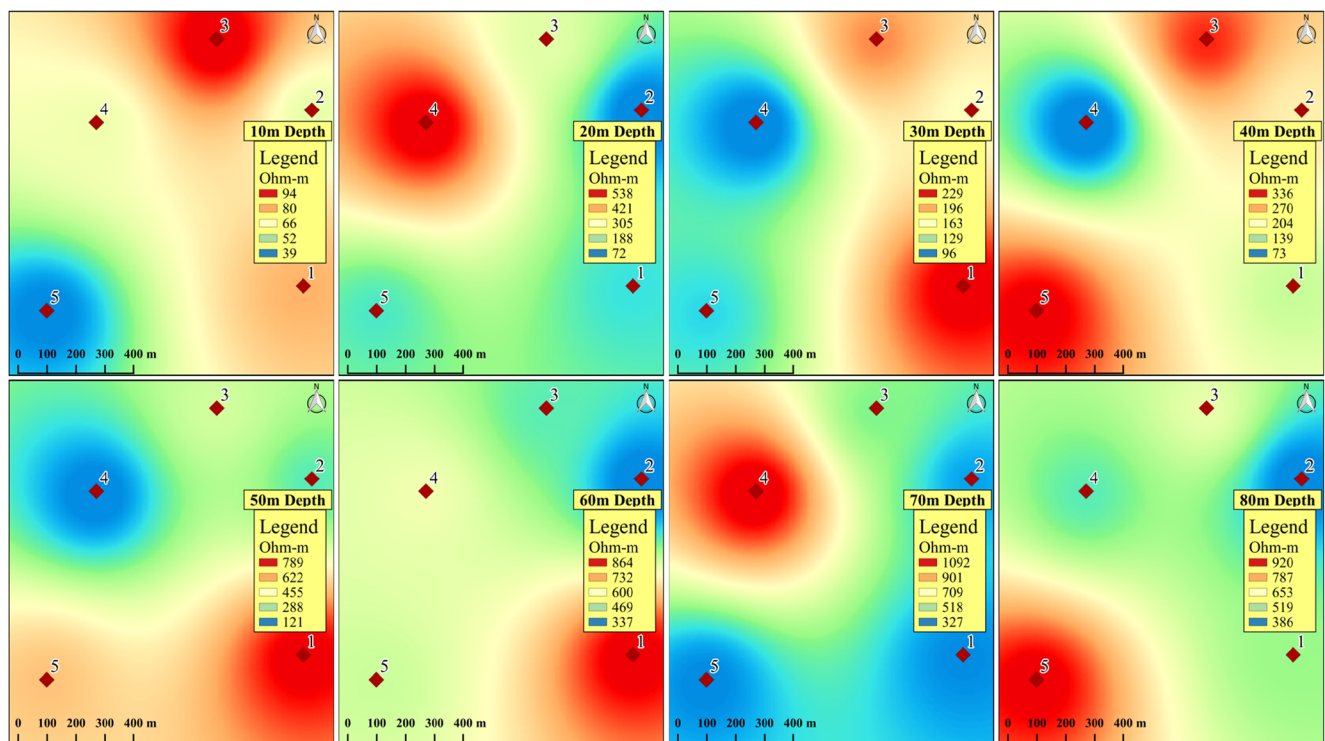
Fig. 5 Depth wise iso-resistivity maps (10 m, 20 m, 30 m, 40, 50 m, 60 m, 70 m, and 80 m) for the study area at 10-m interval
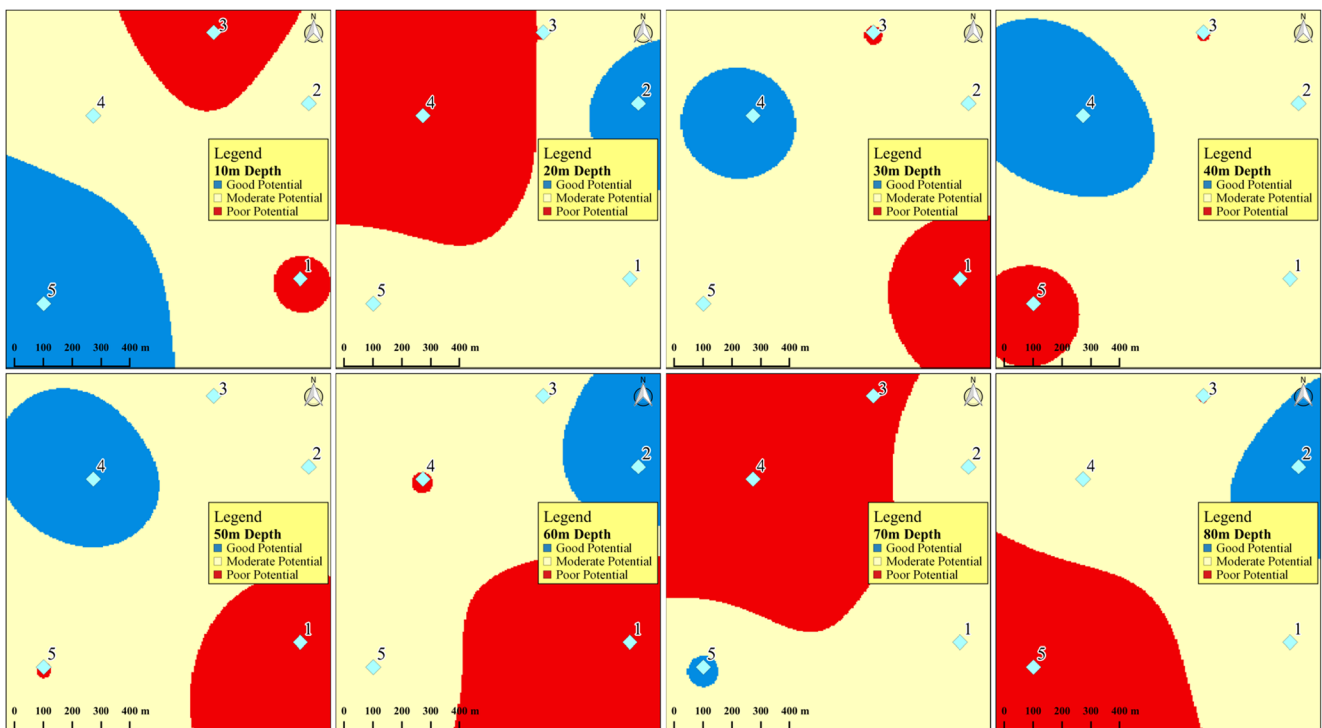
Fig. 6 Reclassified iso-resistivity layers

Iron (Fe)

Iron is the most copious transition element in the Earth's crust and is also probably the most well-known metal in biologic systems. The concentration of total Fe varied between 0.061 and 0.72 ppm with a mean concentration of 0.29 ppm. Spatial distribution (Fig. 8 (Fe)) illustrated in the west to northwestern parts of the study area recorded higher values. Moderately significant values are observed in the central part and low values observed in the southern part of the study area. The BIS (2012) guideline value of Fe for drinking water is 0.3 ppm which makes 40% of groundwater samples as contaminated by Fe.

Fig. 7 The plot shows the box and whisker of the analytical results
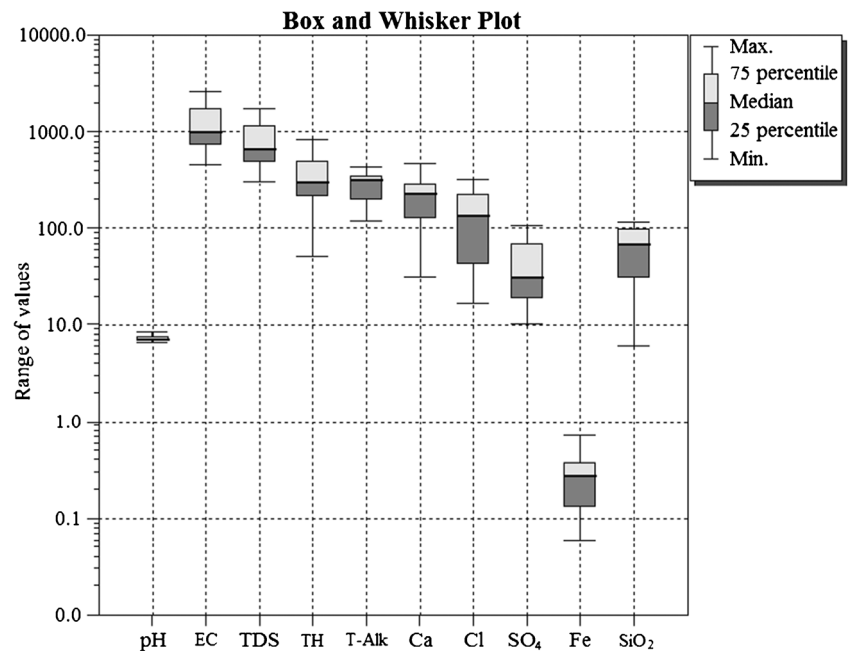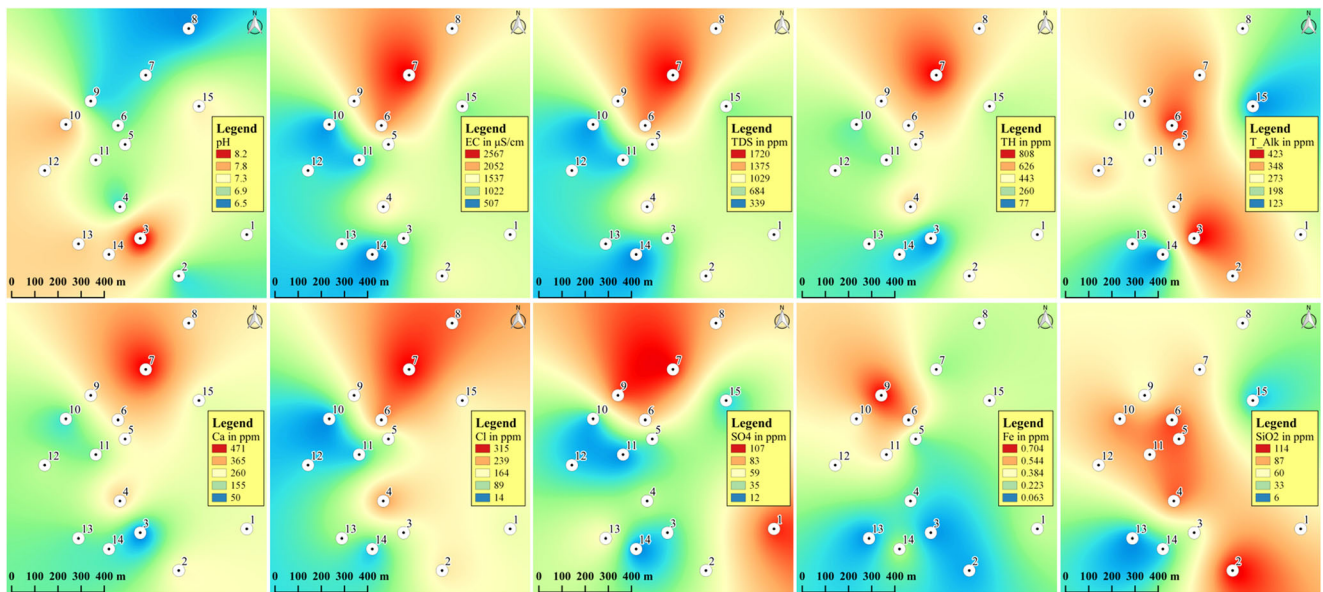
Fig. 8 Spatial distribution of pH, EC, TDS, TH, T-Alk, Ca, Cl, SO_4, Fe, and SiO_2

Silica (SiO_2)

The total silicate concentration varied between 6 and 116 ppm with a mean of 67 ppm. The samples 2, 4, 5, and 6 (Fig. 8 (SiO_2)) of the study area recorded higher SiO_2 concentration of above 100 ppm; however, there is no threshold value for SiO_2 as per the WHO (2008) and BIS (2012) drinking water guidelines.

Analytical hierarchy process

The iso-resistivity and spatial distribution maps were reclassified based on the desired apparent resistivity values and WHO and BIS guideline values as shown in the Tables 10 and 11 with assigned weights for each layer. Relatively low apparent resistivity values are desired for the identification of groundwater potential zones. Accordingly, acceptable limits of each parameter are
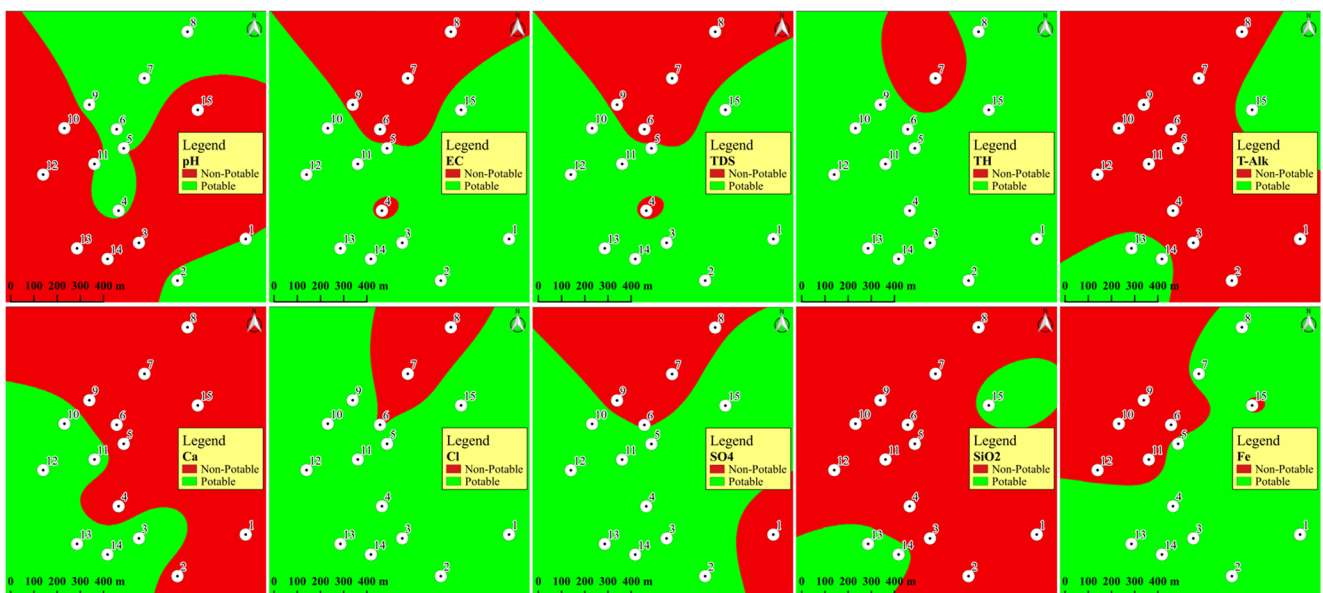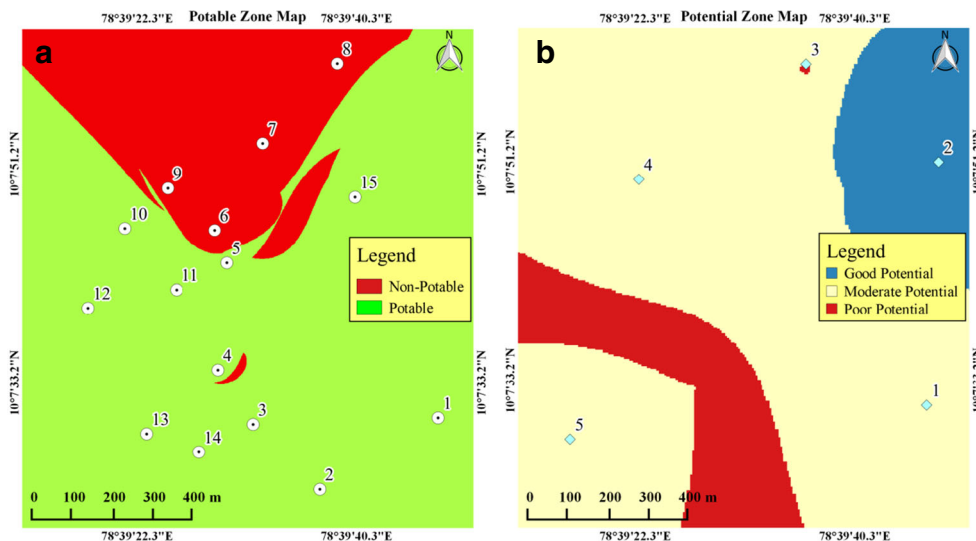

Fig. 9 Reclassified layers of pH, EC, TDS, TH, T-Alk, Ca, Cl, SO_4, Fe, and SiO_2 based on guideline values

Fig. 10 **a** Map showing the potable groundwater zone. **b** Map showing the groundwater potential zone

proposed by the WHO and BIS as potable water guideline values were taken as desirable values for potable groundwater zone identification. In order to assign the weightage to each reclassified layer, the AHP was done with the help of pairwise comparison matrix (Tables 4, 5, and 7) and the consistency ratios for assigned weights are maintained as below 0.1 (Table 9) (Saaty 1980). The normalized eigenvector for comparison matrix of iso-resistivity and spatial distribution layer are given in the Tables 6 and 8. The resulting

maps of potable and potential groundwater zones are shown in Figs. 10a, b, in which 23% of the northern part is denoted by non-potable groundwater and 12.3% of south to western stretch is poor potential groundwater zone in the total study area. These maps were combined to create the potable groundwater potential zone map (Fig. 11a) using a combine grid tool in the integrated saga module of Qgis, and the zonal statistics were illustrated as pie chart (Fig. 11b) and tabulated in Table 12.

Fig. 11 **a** Map showing the potable groundwater potential zone. **b** Pie chart showing the percentage of all the classified zones in the study area
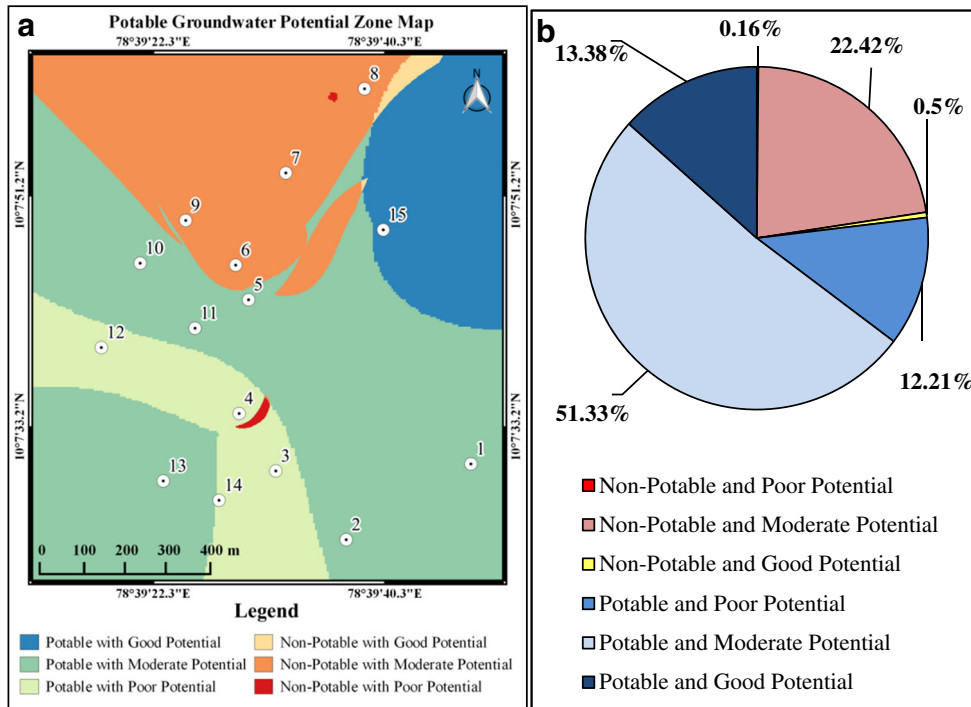
Table 12   Calculated area of each class in the PGWP zone map

Sl. no.	Class	Area (m^2)	in %
1	Non-potable and poor potential	1697	0.16
2	Non-potable and moderate potential	245,320	22.42
3	Non-potable and good potential	5513	0.50
4	Potable and poor potential	133,552	12.21
5	Potable and moderate potential	561,621	51.33
6	Potable and good potential	146,436	13.38

Conclusion

The relatively low apparent resistivity values obtained from the study area reveals the saturation condition of subsurface rock formation, and it lead to the identification of groundwater potential regions. The northeastern part is having good potential, whereas west to south are having poor potential and all other regions found moderate potential. The good potential zone is about 14% and poor potential zone is about 12% in the total study area, the remaining 74% is having moderate potential for groundwater. In many groundwater samples, the physicochemical parameters such as EC, TDS, TH, T-Alk, Ca, Cl, and Fe values exceeded the guideline values proposed by WHO and BIS for drinking. However, pH and SO_4 are found to be within the limits. The overall potable zone map shows that the 23% in northern part is unsuitable for drinking and 77% of all other parts are holding potable groundwater. The AHP was successfully employed for the geophysical and geochemical data to identify the potable groundwater potential zone. The combined analysis of AHP layers shows that 51.33% fall in potable groundwater with moderate potential, 22.42% of non-potable groundwater with moderate potential, and 13.38% of potable groundwater with good potential. Poor potential with non-potable groundwater zone is found in the central part of the study area, and it is about 0.16% of the total area. Non-potable with good potential area is about 0.5%, which is found in the northwestern part of the study area. Rainwater harvesting and artificial recharging of groundwater must be implemented in the poor potential zones and non-potable regions to improve the water level and water quality for the sustainable development of the study area. This new comprehensive method using AHP is able to reduce the uncertainties in the identification of potable groundwater potential zones in complex geological regions. This methodology can be adopted further with different combination of remote sensing layers to precisely identify potable as well as potential groundwater zone in regional and local scale. GIS enabled with AHP is a great advance in hydrogeological studies which reduces the difficulty of problems faced by the researchers all over the world.

Compliance with ethical standards

Conflict of interest   The authors declare that they have no conflict of interest.

References

Ajin RS, Jacob MK, Vinod PG (2014) Tsunami vulnerability mapping using remote sensing and GIS techniques: a case study of Kollam District, Kerala, India. Iranian J Earth Sci 6(1):43–50 http://www.researchgate.net/publication/269169047

APHA (1995) Standard methods for the examination of water and wastewater, 19th edn. American Public Health Association, New York

Appelo T, Postma D (2005) Geochemistry, Groundwater and Pollution. A.A. 1996

BIS (2012) Specification for drinking water IS: 10500:1991. Bureau of Indian Standards, New Delhi

Cabrera JS, Lee HS (2019) Flood-prone area assessment using GIS-based multi-criteria analysis: a case study in Davao Oriental, Philippines. Water 11(11):2203. https://doi.org/10.3390/w11112203

Central Groundwater Board (CGWB) (2008) District groundwater brochure of Sivagangai, Tamil Nadu

Chandra S, Auken E, Maurya PK, Ahmed S, Verma SK (2019) Large scale mapping of fractures and groundwater pathways in crystalline hardrock by AEM. Sci Rep 9(1):1–11. https://doi.org/10.1038/s41598-018-36153-1

Chandrasekar N, Selvakumar S, Srinivas Y, John Wilson JS, Simon Peter T, Magesh NS (2013) Hydrogeochemical assessment of groundwater quality along the coastal aquifers of southern Tamil Nadu, India. Environ Earth Sci 71(11):4739–4750. https://doi.org/10.1007/s12665-013-2864-3

Chidambaram S, Bala Krishna Prasad M, Manivannan R, Karmegam U, Singaraja C, Anandhan P, Prasanna MV, Manikandan S (2012) Environmental hydrogeochemistry and genesis of fluoride in groundwaters of Dindigul district, Tamilnadu (India). Environ Earth Sci 68:333–342. https://doi.org/10.1007/s12665-012-1741-9

Chidambaram S, Anandhan P, Prasanna MV, Srinivasamoorthy K, Vasanthavigar M (2013) Major ion chemistry and identification of hydrogeochemical processes controlling groundwater in and around Neyveli Lignite Mines, Tamil Nadu, South India. Arab J Geosci 6(9):3451–3467. https://doi.org/10.1007/s12517-012-0589-3

Chung SY, Rajendran R, Venkatramana S, Sekar S, Ranganathan PC, Oh YY, Elzain HE (2020) Processes and characteristics of hydrogeochemical variations between unconfined and confined aquifer systems: a case study of the Nakdong River Basin in Busan City, Korea. Environ Sci Pollut Res 27:10087–10102. https://doi.org/10.1007/s11356-019-07451-6

Coker JO, Makinde V, Olowofela JA (2009) Geophysical investigation of groundwater potentials of Oke-Badan estate, Ibadan, southwestern, Nigeria. Proceedings of 3rd International Conference on Science and National Development University of Agric. Abeokuta, p 119

Conrad O, Bechtel B, Bock M, Dietrich H, Fischer E, Gerlitz L, Wehberg J, Wichmann V, Böhner J (2015) System for Automated Geoscientific Analyses (SAGA) v. 2.1.4. Geosci Model Dev 8(7):1991–2007. https://doi.org/10.5194/gmd-8-1991-2015

Dasgupta AM, Purohit KM (2001) Status of surface and groundwater quality of Mandiakadar-part II: agricultural utilities. Pollut Res 20(2):219–225

Fenta AA, Kifle A, Gebreyohannes T, Hailu G (2014) Spatial analysis of groundwater potential using remote sensing and GIS-based multi-criteria evaluation in Raya Valley, northern Ethiopia. Hydrogeol J 23(1):195–206. https://doi.org/10.1007/s10040-014-1198-x

Gangadharan R, Nila RP, Vinoth S (2016) Assessment of groundwater vulnerability mapping using AHP method in coastal watershed of shrimp farming area. Arab J Geosci 9(2):1–14. https://doi.org/10.1007/s12517-015-2230-8

Gnanachandrasamy G, Ramkumar T, Venkatramanan S, Vasudevan S, Chung SY, Bagyaraj M (2015) Accessing groundwater quality in lower part of Nagapattinam district, Southern India: using hydrogeochemistry and GIS interpolation techniques. Appl Water Sci 5(1):39–55. https://doi.org/10.1007/s13201-014-0172-z

Gnanachandrasamy G, Zhou Y, Bagyaraj M, Venkatramanan S, Ramkumar T, Wang S (2018) Remote sensing and GIS based groundwater potential zone mapping in Ariyalur District, Tamil Nadu. J Geol Soc India 92(4):484–490. https://doi.org/10.1007/s12594-018-1046-z

Habberjam GM (1972) The effects of anisotropy on square array resistivity measurements. Geophys Prospect 20:249–266

Habberjam GM (1975) Apparent resistivity, anisotropy and strike measurements. Geophys Prospect 23:211–247

Habberjam GM (1979) Apparent resistivity observations and the use of square array techniques. In: Saxov S and Flathe H (eds) Geoexploration Monographs. series 1, no 9, pp 1–152

Habberjam GM, Watkins GE (1967) The use of a square configuration in resistivity prospecting. Geophys Prospect 15:221–235

Hem JD (1991) Study and interpretation of the chemical characteristics of natural waters. Book 2254, 3rd edn. Scientific Publishers, Jodhpur

Ibrahim I, Asmawi MZ, Jaafar S (2017) Temporal geospatial shorelines changes analysis in Klang coastal area. Adv Sci Lett 23(7):6362–6366. https://doi.org/10.1166/asl.2017.9270

Juahir H, Zain SM, Yusoff MK, Hanidza TIT, Armi ASM, Toriman ME, Mokhtar M (2011) Spatial water quality assessment of Langat River Basin (Malaysia) using environmetric techniques. Environ Monit Assess 173(1–4):625–641. https://doi.org/10.1007/s10661-010-1411-x

Kanagaraj G, Suganthi S, Elango L, Magesh NS (2019) Assessment of groundwater potential zones in Vellore district, Tamil Nadu, India using geospatial techniques. Earth Sci Inf 12(2):211–223. https://doi.org/10.1007/s12145-018-0363-5

Karanth KR (1997) Groundwater assessment, development and management. Tata McGraw-Hill, New Delhi

Khurshid SH, Hasan N, Zaheeruddin (2002) Water quality status and environmental hazards in parts of Yamuna–Karwan sub-basin of Aligarh–Mathura district, Uttar Pradesh, India. J Appl Hydrol 14(4):30–37

Krishna kumar S, Logeshkumaran A, Magesh NS, Godson PS, Chandrasekar N (2014) Hydro-geochemistry and application of water quality index (WQI) for groundwater quality assessment, Anna Nagar, part of Chennai City, Tamil Nadu, India. Appl Water Sci 5(4):335–343. https://doi.org/10.1007/s13201-014-0196-4

Machiwal D, Jha MK, Mal BC (2011) Assessment of groundwater potential in a semi-arid region of India using remote sensing, GIS and MCDM techniques. Water Resour Manag 25(5):1359–1386. https://doi.org/10.1007/s11269-010-9749-y

Majumdar D, Gupta N (2000) Nitrate pollution of groundwater and associated human health disorders, India. J Environ Health 42(1):28–39

Mohamed AS, Thirumaran G, Arumugam R, Ragupathi RKR, Anantharaman P (2009) Physico- chemical parameters of holy places Agnitheertham and Kothandaramar Temple; southeast coast of India. Am Eurasian J Sci Res 4(2):108–116

Mondal S (2012) Remote sensing and GIS based ground water potential mapping of Kangshabati irrigation command area, West Bengal. J Geogr Nat Disasters 01(01):1–8. https://doi.org/10.4172/2167-0587.1000104

Pinto D, Shrestha S, Babel MS, Ninsawat S (2017) Delineation of groundwater potential zones in the Comoro watershed, Timor Leste using GIS, remote sensing and analytic hierarchy process (AHP) technique. Appl Water Sci 7(1):503–519. https://doi.org/10.1007/s13201-015-0270-6

Pulle JS, Khan AM, Ambore NE, Kadam DD, Pawar SK (2005) Assessment of groundwater quality of Nanded City. Pollut Res 24(3):657–660

Rahimi D, Mokarram M (2012) Assessing the groundwater quality by applying fuzzy logic in GIS environment-a case study in Southwest Iran. Agris On-Line Pap Econ Inform 2(3):1798–1806. https://doi.org/10.6088/ijes.002020300063

Ramachandran A, Sivakumar K, Shanmugasundharam A, Sangunathan U, Krishnamurthy RR (2020) Evaluation of potable groundwater zones identification based on WQI and GIS techniques in Adyar River basin, Chennai, Tamilnadu, India. Acta Ecol Sin. https://doi.org/10.1016/j.chnaes.2020.02.006

Ravindran A, A (2012) Azimuthal square array configuration and groundwater prospecting in quartzite Terrian at Edaikkal, Ambasamudram, Tirunelveli. Res J Earth Sci 4(2):49–55

Ravindran A, A, Muthusamy S, Moorthy G, Vinothkingston J, Mohana P (2018) Groundwater – quartzite area study using square array method in Puthukottai, Tuticorin District, Tamilnadu, India. Int J Adv Multidiscip Sci Res 1(10):43–54. https://doi.org/10.31426/ijamsr.2018.1.10.1016

Saaty TL (1980) The analytic hierarchy process. McGraw-Hill, New York, p 278

Sawyer CN, McCarty PL (1978) Chemistry for Environmental Engineering, 3rd edn. McGraw-Hill Book Co., New York

Selvam S, Venkatramanan S, Singaraja C (2015) A GIS-based assessment of water quality pollution indices for heavy metal contamination in Tuticorin corporation, Tamilnadu, India. Arab J Geosci 8(12):10611–10623. https://doi.org/10.1007/s12517-015-1968-3

Selvam S, Venkatramanan S, Chung SY, Singaraja C (2016) Identification of groundwater contamination sources in Dindugal district of Tamil Nadu, India using GIS and multivariate statistical analyses. Arab J Geosci 9(5). https://doi.org/10.1007/s12517-016-2417-7

Sivakumar K, Priya J, Muthusamy S, Saravanan P, Jayaprakash M (2016) Spatial diversity of major ionic absorptions in groundwater : recent study from the industrial region of Tuticorin, Tamil, Nadu, India. EnviroGeoChemica Acta 3(1):138–147

Sivakumar K, Muthusamy S, Jayaprakash M, Mohana P, Sudharson ER (2017) Application of post classification in landuse & landcover strategies at north Chennai industrial area. J Adv Res Geo Sci Remote Sens 4(3&4):1–13

Subba Rao N (2006) Seasonal variation of groundwater quality in a part of Guntur district, Andhra Pradesh, India. Environ Geol 49:413–429

Sujatha D, Redd RB (2003) Quality characterization of groundwater in the south-eastern part of the Ranja Reddy district, Andhra Pradesh, India. Environ Geol 44(5):579–586

Venkatramanan S, Chung SY, Kim TH, Prasanna MV, Hamm SY (2015) Assessment and distribution of metals contamination in groundwater: a case study of Busan City, Korea. Water Qual Expo Health 7(2):219–225. https://doi.org/10.1007/s12403-014-0142-6

Venkatramanan S, Chung SY, Selvam S, Lee SY, Elzain HE (2017) Factors controlling groundwater quality in the Yeonjegu District of Busan City, Korea, using the hydrogeochemical processes and fuzzy GIS. Environ Sci Pollut Res 24(30):23679–23693. https://doi.org/10.1007/s11356-017-9990-5

WHO (1996) Trace elements in human nutrition and health. Geneva, ISBN: 9241545143

WHO (2008) Guidelines for drinking water quality. vol 1. Recommendations, 3rd edn. WHO, Geneva, p 515

Zaporozec A (1972) Graphical interpretation of water quality data. Groundwater 10(2):32–43